# CrystEngComm

Accepted Manuscript

ROYAL SOCIETY OF CHEMISTRY

www.rsc.org/crystengcomm

Journal Name RSCPublishing

ARTICLE

# Self Assembly of Carboxylate/Alcoholate Functionalized Ring-shape Phosphomolybdates

Cite this: DOI: 10.1039/x0xx00000x

Received 00th January 2012,
Accepted 00th January 2012

DOI: 10.1039/x0xx00000x

www.rsc.org/

Donghui Yang,[a] Yanfen Liang,[a] Pengtao Ma,[a] Suzhi Li,[b] Jingping Wang*[a] and Jingyang Niu*[a]

We report a simple and efficient approach to incorporate organic groups into polymolybdates by reaction of $H_3PO_3$ with $Na_2MoO_4{\cdot}2H_2O/(NH_4)_6Mo_7O_{24}{\cdot}4H_2O$ and organic components in aqueous medium. The carboxylate and alcoholate ligands were covalently attached to the $[HPMo_6O_{21}]^{2-}$ cluster to generate a series of inorganic–organic hybrid phosphomolybdates. Thus, depending on the successful synthesis of these structures, it could be possible to obtain a variety of these hybrids through a great deal of rational structural design using the ligand control, which is rarely known in traditional "one-pot" polyoxometalate (POM) synthesis.

## Introduction

The interest in inorganic-organic hybrids constructed from POMs in recent years is based on their fascinating structural, physical and chemical properties.[1] According to the nature of the interaction between the organic and inorganic components, these hybrids have been defined as covalent and noncovalent POM-based hybrids.[2] So far, the covalent grafting of organic components onto POM clusters is an active field of research because of their unique electronic, catalytic and photonic properties.[3] These attractive features have led to intense investigation of their synthetic strategy, and the advantage of covalent grafting in terms of stability and structure control underlines the exceptionally great efforts in synthetic interest. For example, the ring-shape hexanuclear heteropolymolybdates which are templated by pyramidal heteroatoms and combined with organic groups have been extensively explored, such as amino acid based derivatives $[XMo_6O_{21}(O_2CRNH_3)_3]^{n-}$ (n = 2, X = $Se^{IV}$, $Te^{IV}$, POH, $PCH_3$, $PC_2H_5$, PH; n = 3, X = $As^{III}$, $Sb^{III}$, $Bi^{III}$; R = $CH_2$, $C_2H_4$, $C_3H_6$, $CHCH_3$, $CH(CH_2)_4NH_2$),[4] phosphorus-containing derivatives $[(O_3PRPO_3)Mo_6O_{18}(H_2O)]^{4-}$ (R = $CH_2$, O), $[Mo_6O_{17}(H_2O)(O_3PCH_2NH_2CH_2PO_3)_2]^{4-}$, $\{(CH_3CO_2)[N(CH_2PO_3)_3]Mo_6O_{17}(OH)\}^{6-}$ and $\{[HN(CH_2PO_3)_2](CH_3CO_2)PMo_6O_{22}\}^{6-}$.[5] So it can be acknowledged that the $Mo_6$ ring can be easily grafted with organic groups. We reasoned that the replacement of amino acid by carboxylic acid or even multicarboxylic acid should be of interest from the view of self-assembly.

The past two decades have viewed the development of carboxylate functionalized isopolymolybdates toward the generation of hybrid materials with vast structural variation and composition.[6] In contrast, the heteropolymolybdates functionalized by multicarboxylic acids are less frequently known. To address this gap, we opted to use hexanuclear polyoxoanions $[XMo_6O_{21}]^{n-}$ (X = HP, Se, n = 2; X = As, n = 3) and carboxylic acids and attempted to discover an efficient approach to enhance the directionality and interaction between two components. This approach had consequently resulted in a wealth of new heteropolymolybdate derivatives[7] and further filled the vacant positions in multi-carboxylic acids functionalized heteropolymolybdates.

In this paper, the synthetic approach is inherited and developed. We have specifically used alcoholate ligand which leads to the generation of a new ring-shape phosphomolybdate *via* the ligand self-directed assembly. Depending on the flexibility and conformational freedom of organic ligands, six compounds $(C_3N_2H_5)_4[Na(H_2O)_3(HPMo_6O_{21})(CH_3CO_2)_3]{\cdot}4H_2O$ (**1**), $(NH_4)_3H_2[HPMo_6O_{21}(O_2CC_6H_4NH_2)_3]{\cdot}9H_2O$ (**2**), $(NH_4)_5[HPMo_6O_{21}\{O_2CC_6H_4(OH)_2\}_3]{\cdot}5H_2O$ (**3**), $(NH_4)_{10}[(HPMo_6O_{21})_2\{O_2C(CH_2)_2CO_2\}_3]{\cdot}6H_2O$ (**4**), $(NH_4)_{10}[(HPMo_6O_{21})_2\{O_2C(CH_2)_4CO_2\}_3]{\cdot}6.5H_2O$ (**5**) and $(NH_4)_5[HPMo_6O_{21}\{N(CH_2CH_2O)_3\}]{\cdot}5.5H_2O$ (**6**) were synthesized and structurally characterized in the solid state. These architectures are extremely susceptible to the organic groups because of inherent nature of organic ligands: acetic acid ($CH_3CO_2H$), m-aminobenzoic acid ($NH_2C_6H_4CO_2H$), 2,4-dihydroxybenzoic acid ($HO_2CC_6H_4(OH)_2$), succinic acid ($HO_2C(CH_2)_2CO_2H$), adipic acid ($HO_2C(CH_2)_4CO_2H$) and triethanolamine ($N(CH_2CH_2OH)_3$).

## Experimental

## Materials and methods

All chemical reagents were purchased from commercial sources and used without further purification. IR spectra were recorded on a Bruker VERTEX 70 IR spectrometer using KBr pellets in the range of 4000–400 $cm^{-1}$. C, H and N elemental analyses were performed on a Perkin-Elmer 2400-II CHNS/O analyzer. XPS spectra were recorded on an Axis Ultra (Kratos, U.K.) photoelectron spectroscope using monochromatic Al *K*α (1486.7 eV) radiation. $^{31}P$ NMR spectra were recorded in 5 mm tubes with 1H decoupling by using a Bruker AC-300 spectrometer operating at 121.5 MHz. $^{31}P$ chemical shifts were referenced to the external standard of 85% $H_3PO_4$. For all compounds, ≈20 mg of sample was dissolved in $D_2O$ (700 μL).

### Synthesis of $(C_3N_2H_5)_4[Na(H_2O)_3(HPMo_6O_{21})(CH_3CO_2)_3]\cdot 4H_2O$ (1)

$Na_2MoO_4\cdot 2H_2O$ (0.73 g, 3.02 mmol) and $CH_3CO_2Na$ (0.25 g, 3.05 mmol) were dissolved in water (10 mL), then $H_3PO_3$ (0.04 g, 0.49 mmol) and imidazole (0.10 g, 1.47 mmol) were added. The pH of this mixture was adjusted to 4.7 by addition of acetic acid, and the reaction mixture was heated at 60 °C for 3 h, cooled, filtered and left to evaporate slowly. Colourless block crystals of **1** appeared after about four weeks. Yield: 0.37 g (65%) for **1** based on imidazole. Elemental analysis calcd (%) for $C_{18}H_{44}N_8Mo_6O_{34}NaP$ (**1**): C 13.98, H 2.87, N 7.25, P 2.00, Mo 37.22; found: C 13.72, H 2.73, N 6.91, P 2.03, Mo 36.81. IR (KBr pellet): 3547(s), 3480(s), 3162(m), 2996(w), 2968(w), 2938(w), 2891(w), 2425(w), 2053(w), 1630(m), 1563(s), 1448(s), 1420(s), 1354(w), 1308(w), 1259(w), 1218(w), 1069(s), 1023(m), 992(w), 932(s), 900(s), 796(s), 688(s), 596(m), 536(m), 518 $cm^{-1}$ (m).

### Synthesis of $(NH_4)_3H_2[HPMo_6O_{21}(O_2CC_6H_4NH_2)_3]\cdot 9H_2O$ (2)

$(NH_4)_6Mo_7O_{24}\cdot 4H_2O$ (1.06 g, 0.86 mmol) was dissolved in water (15 mL), then $H_3PO_3$ (0.08 g, 0.98 mmol) and m-aminobenzoic acid (0.41g, 3.00 mmol) were added. The reaction mixture was stirred approximately 2 h at 70 °C to result in a yellow-brown solution, cooled, filtered and left to evaporate slowly. Brown block crystals of **2** appeared after about four weeks. Yield: 0.20 g (13%) for **2** based on $H_3PO_3$. Elemental analysis calcd (%) for $C_{21}H_{51}N_6Mo_6O_{36}P$ (**2**): C 16.06, H 3.27, N 5.35, P 1.97, Mo 36.66; found: C 15.86, H 3.28, N 4.91, P 2.04, Mo 37.03. IR (KBr pellet): 3415(s), 3177(s), 3033(s), 2863(s), 2621(m), 2417(w), 1620(m), 1552(s), 1452(m), 1406(s), 1161(w), 1078(s), 1009(w), 933(s), 896(s), 795(w), 763(m), 672(s), 567(m), 536(m), 458 $cm^{-1}$ (m).

### Synthesis of $(NH_4)_5[HPMo_6O_{21}\{O_2CC_6H_4(OH)_2\}_3]\cdot 5H_2O$ (3)

Same procedure as for **2**, (0.46 g, 2.99 mmol) 2,4-dihydroxybenzoic acid instead of m-aminobenzoic acid. Pale yellow block crystals of **3** appeared after about four weeks. Yield: 0.36g (23%) for **3** based on $H_3PO_3$. Elemental analysis calcd (%) for $C_{21}H_{49}N_5Mo_6O_{38}P$ (**3**): C 15.90, H 3.11, N 4.42, P 1.95, Mo 36.29; found: C 15.45, H 3.51, N 4.21, P 2.01, Mo 36.57. IR (KBr pellet): 3435(s), 3168(s), 1632(s), 1605(s), 1552(s), 1516(m), 1459(s), 1400(s), 1300(m), 1248(m), 1161(m), 1069(s), 1001(w), 978(w), 930(s), 899(s), 784(m), 678(s), 636(s), 568(m), 538 $cm^{-1}$ (m).

### Synthesis of $(NH_4)_{10}[(HPMo_6O_{21})_2\{O_2C(CH_2)_2CO_2\}_3]\cdot 6H_2O$ (4)

Same procedure as for **2**, 0.18 g (1.53 mmol) succinic acid instead of m-aminobenzoic acid. Colourless block crystals of **4** appeared after about four weeks. Yield: 0.38 g (31%) for **4** based on $H_3PO_3$. Elemental analysis calcd (%) for $C_{12}H_{66}N_{10}Mo_{12}O_{60}P_2$ (**4**): C 5.71, H 2.64, N 5.55, P 2.45, Mo 45.61; found: C 5.40, H 3.26, N 5.19, P 2.59, Mo 46.02. IR (KBr pellet): 3479(s), 3153(s), 2415(w), 1626(m), 1562(s), 1402(s), 1236(w), 1159(w), 1080(s), 1007(w), 932(s), 899(s), 673(s), 569(m), 540 $cm^{-1}$(m).

### Synthesis of $(NH_4)_{10}[(HPMo_6O_{21})_2\{O_2C(CH_2)_4CO_2\}_3]\cdot 6.5H_2O$ (5)

Same procedure as for **2**, (0.22 g, 1.51 mmol) adipic acid instead of m-aminobenzoic acid. Colourless block crystals of **5** appeared after about four weeks. Yield: 0.44 g (34%) for **5** based on $H_3PO_3$. Elemental analysis calcd (%) for $C_{18}H_{79}N_{10}Mo_{12}O_{60.5}P_2$ (**5**): C 8.26, H 3.04, N 5.35, P 2.37, Mo 43.99; found: C 8.26, H 3.34, N 5.26, P 2.46, Mo 44.21. IR (KBr pellet): 3459(s), 3174(s), 1629(w), 1556(s), 1408(s), 1336(w), 1074(s), 1003(w), 928(s), 896(s), 676(s), 568(m), 539 $cm^{-1}$ (m).

### Synthesis of $(NH_4)_5[HPMo_6O_{21}\{N(CH_2CH_2O)_3\}]\cdot 5.5H_2O$ (6)

Same procedure as for **2**, (0.20 g, 1.34 mmol) triethanolamine instead of m-aminobenzoic acid. Pale yellow block crystals of **6** appeared after about four weeks. Yield: 0.41 g (33%) for **6** based on $H_3PO_3$. Elemental analysis calcd (%) for $C_6H_{44}Mo_6N_6O_{29.5}P$ (**6**): C 5.63, H 3.47, N 6.57, P 2.42, Mo 45.01; found: C 5.86, H 3.84, N 6.76, P 2.45, Mo 45.38. IR (KBr pellet): 3435(s), 3178(s), 3086(s), 2878(s), 2415(w), 2075(w), 1637(m), 1437(s), 1403(s), 1269(w), 1216(w), 1110(m), 1078(s), 1000(m), 922(s), 895(s), 637(s), 557(s), 521 $cm^{-1}$ (s).

## X-ray crystallography

A summary of crystallographic data and structural refinements for **1–6** is given in Table 1. Intensity data were collected at 293 or 296 K on a Bruker APEX-II CCD diffractometer for **1–6** using graphite-monochromated Mo Kα radiation (λ = 0.71073 Å). Routine Lorentz and polarization corrections were applied and an absorption correction was performed using the SADABS program. Direct methods were used to solve the structure and refined by full-matrix least-squares on $F^2$ using the SHELXTL-97 program package. Non-hydrogen atoms were refined anisotropically. Moreover, $NH_4^+$ and lattice $H_2O$ could not be distinguished based on electron densities, thus we determine the lattice water molecules and $NH_4^+$ ions by elemental analysis. CCDC reference numbers 951524–951528 for **1–5** and 951523 for **6**, respectively. These data can be obtained free of charge from the Cambridge Crystallographic Data Centre via www.ccdc.cam.ac.uk/data_ request/cif.

**Table 1**. Crystallographic Data and Structural Refinements for **1–6**

| | 1 | 2 | 3 |
|---|---|---|---|
| Empirical formula | $C_{18}H_{44}N_8Mo_6O_{34}NaP$ | $C_{21}H_{51}N_6Mo_6O_{36}P$ | $C_{21}H_{49}N_5Mo_6O_{38}P$ |
| Formula weight | 1546.21 | 1570.37 | 1586.24 |
| Space group | *Pnma* | *C2/c* | *P-1* |

| | | | |
|---|---|---|---|
| Crystal system | Orthorhombic | Monoclinic | Triclinic |
| a / Å | 14.932(5) | 24.950(8) | 12.375(2) |
| b / Å | 13.158(4) | 21.344(7) | 12.611(3) |
| c / Å | 23.575(7) | 21.084(6) | 18.842(4) |
| α / deg | 90 | 90 | 79.892(4) |
| β / deg | 90 | 120.510(6) | 89.735(4) |
| γ / deg | 90 | 90 | 70.484(3) |
| V / Å$^3$ | 4632(2) | 9673(5) | 2723.9(10) |
| Z | 4 | 8 | 2 |
| Goodness-of-fit on F$^2$ | 1.058 | 1.035 | 1.062 |
| R$_1$,wR$_2$ [I>2σ(I)] | 0.0323 0.0852 | 0.0431 0.1046 | 0.0504 0.1708 |
| R$_1$,wR$_2$[all data] | 0.0356 0.0874 | 0.0698 0.1210 | 0.0625 0.1794 |

| | 4 | 5 | 6 |
|---|---|---|---|
| Empirical formula | $C_{12}H_{66}N_{10}Mo_{12}O_{60}P_2$ | $C_{18}H_{79}N_{10}Mo_{12}O_{60.5}P_2$ | $C_6H_{44}Mo_6N_6O_{29.5}P$ |
| Formula weight | 2523.95 | 2617.12 | 1279.08 |
| Space group | *P2(1)/m* | *P2(1)/n* | *Pca2(1)* |
| Crystal system | Monoclinic | Monoclinic | Orthorhombic |
| a / Å | 15.184(6) | 18.1471(18) | 14.3564(12) |
| b / Å | 17.929(7) | 26.828(3) | 13.8963(12) |
| c / Å | 16.115(6) | 19.2959(19) | 18.4197(15) |
| α / deg | 90 | 90 | 90 |
| β / deg | 117.472(6) | 115.157(2) | 90 |
| γ / deg | 90 | 90 | 90 |
| V / Å$^3$ | 3893(3) | 8503.1(15) | 3674.7(5) |
| Z | 2 | 4 | 4 |
| Goodness-of-fit on F$^2$ | 1.043 | 1.010 | 1.037 |
| R$_1$,wR$_2$ [I>2σ(I)] | 0.1098 0.3193 | 0.0685 0.1587 | 0.0307 0.0825 |
| R$_1$,wR$_2$[all data] | 0.1559 0.3417 | 0.1712 0.1880 | 0.0325 0.0837 |

## Results and discussion

### Structural descriptions

Compounds **1–5** have been synthesized by a simple one-pot reaction of $Na_2MoO_4·2H_2O/(NH_4)_6Mo_7O_{24}·4H_2O$, $H_3PO_3$ and carboxylic acids in aqueous solution. These compounds contain the common $[HPMo_6O_{21}]^{2-}$ polyoxoanion, which is built up of six $\{MoO_6\}$ octahedra alternately sharing edges and corners connected into a ring centered by a central $\{PO_3\}$ group (Fig. S1, ESI). The center P coordinates to three $\mu_3$-O atoms and is situated on the plane of six-numbered $Mo_6$ ring. In addition, this unit is difficult to isolate as an individual cluster and only stable in the presence of organic components, which possesses six potential reactive sites and easily coordinate with oxygen-containing ligands. Herein, different organic ligands were used to explore the assembly process of the POM frameworks. Also, it should be noted the geometry and connectivity of a ligand dictate the structure of resulting POM. Our preliminary experimental exploration showed that the self-assembly process of polyanion in solution is strongly affected by organic ligands. By adjusting the geometry, length and functional-group of ligands, it is capable of tuning the size, shape, and internal structure of final product.

The structure of $[Na(H_2O)_3(HPMo_6O_{21})(CH_3CO_2)_3]^{4-}$ (**1a**) is shown in Figure 1a. Three outward acetate ligands graft to three groups of edge-sharing $\{MoO_6\}$ octahedra via six carboxyl oxygen atoms respectively. The $[Na(H_2O)_3]^+$ ion displays the distorted octahedral geometry, which is defined by two O atoms from the acetate ligands and one $\mu_2$-O atom from the $[HPMo_6O_{21}]^{2-}$ cluster. Additionally, acetate and $[Na(H_2O)_3]^+$ ion are all situated on the same side of the six-numbered $\{Mo_6\}$ ring plane. The polyoxoanions $[HPMo_6O_{21}(O_2CC_6H_4NH_2)_3]^{5-}$ (**2a**) and $[HPMo_6O_{21}\{O_2CC_6H_4(OH)_2\}_3]^{5-}$ (**3a**) (Fig. 1b and 1c) are essentially identical to that previously reported for carboxylate functionalized heteropolymolybdates.[4,7,8]

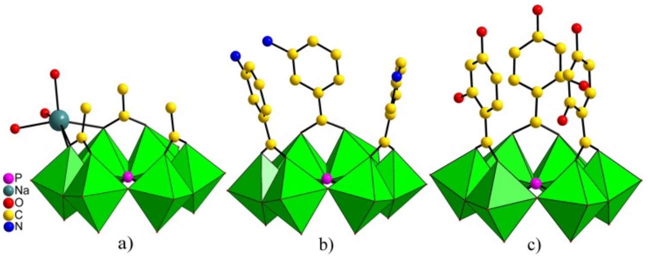

**Fig. 1** Polyhedral/ball-and-stick representation of polyanions **1–3** (a-c). ($MoO_6$ octahedra: green. Hydrogen atoms are omitted for clarity).

The choice of appropriate ligands has to be considered in order to produce remarkable architectures, because organic groups contain the information required (singular coordination requirement) for the successful assembly. Aliphatic dicarboxylic acids were chosen as the suitable ligands to investigate the possibility of synthesizing new cluster species. This approach resulted in two new POM-based hybrids **4** and **5**. Compared with compounds **1–3**, the structures of **4** and **5** seem to be three dicarboxylate linkers sandwiched by two $[HPMo_6O_{21}]^{2-}$ units (Fig. 2). Specifically, both $[HPMo_6O_{21}]^{2-}$ clusters arrange in a face-to-face mode, in which the dicarboxylate linkers act as pillars within the scaffold structures of **4** and **5**. Interestingly, dicarboxylate ligands as flexible hinges adopt concerted screwed torsion to coordinate with $[HPMo_6O_{21}]^{2-}$ unit due to the distort of carbon chains, thus the upper and lower $[HPMo_6O_{21}]^{2-}$ clusters exhibit the unsymmetric superimposed structures. It is noteworthy that the void space of target structures could be possibly enlarged by increasing the length of the dicarboxylate linker units in the similar dimer systems.[7b, c]

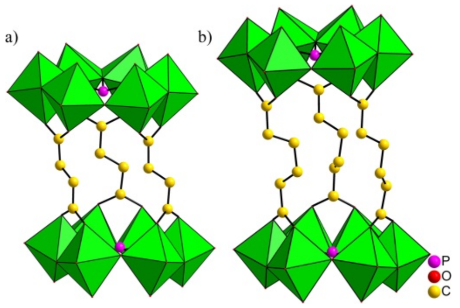

**Fig. 2** Polyhedral/ball-and-stick representation of polyanions **4** and **5** (a and b). ($MoO_6$ octahedra: green. Hydrogen atoms are omitted for clarity).

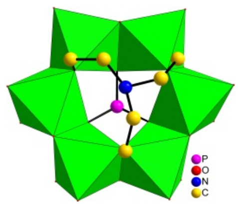

**Fig. 3** Polyhedral/ball-and-stick representation of polyanion **6**. ($MoO_6$ octahedra: green. Hydrogen atoms are omitted for clarity).

Inspired by the structures of **1–5**, in which dicarboxylate ligands is directly anchored to the metallic centers by substituting the oxo group of $\{Mo_6\}$ ring, we investigate the possibility that $[HPMo_6O_{21}]^{2-}$ cluster could be grafted on other type of oxygen-containing organic ligand. This essential property has facilitated our efforts to explore the effect of the organic group as a structure directing ligand for making specific framework in the reaction system. It is very interesting to note that the use of triethanolamine ligand constitutes a new type of isomerism in metal oxide cluster science. As shown in Figure 3, the polyoxoanion $[HPMo_6O_{21}\{N(CH_2CH_2O)_3\}]^{5-}$ (**6a**) consists of a heteroatom P surrounded by a ring of six $\{MoO_6\}$ octahedra sharing edges. Each hydroxy group of triethanolamine ligand is bound to two edge-sharing Mo atoms on the same side of the ring. The central P atom, located slightly below the plane of six Mo atoms, is coordinated to three $\mu_3$-oxo groups which is on the different side of the ring as the triethanolamine ligand (Fig. S2, ESI). In comparison with $\{PMo_6\}$ unit in **1–5**, some obvious distinctions are observed in **6**. In this $[HPMo_6O_{21}]^{2-}$ cluster, it can be clearly seen that six $\{MoO_6\}$ octahedra all display the distorted octahedra coordination geometry, and this connection mode of $[HPMo_6O_{21}]^{2-}$ unit is rarely known in POM chemistry. Obviously, the triethanolamine functionalized $[HPMo_6O_{21}]^{2-}$ cluster is resemble to that of single-side organically functionalized Anderson-Type POMs.[10]

## IR Spectra

IR spectra were used to investigate the structural characters of compounds **1–6** (Fig. S3, ESI). Compounds **1–5** show similar characteristic patterns in the region between 450 and 1650 $cm^{-1}$, indicating that the polyanions in **1–5** have the same basic framework, which are in good agreement with the results of single-crystal X-ray structural analyses. The characteristic peaks at strong absorption bands in the range of 933–895 $cm^{-1}$ are assigned to the vibrations of terminal Mo=O units and those in the range of 688–635 $cm^{-1}$ are assigned to the vibrations of Mo–O–Mo groups. The P–O vibration bands in **1–6** appear at 1069, 1078, 1069, 1080, 1074 and 1078 $cm^{-1}$, respectively. More specifically, the ν(C=O) bands appear in the region 1632–1400 $cm^{-1}$, demonstrating the grafting of organic ligands onto the surface of POMs. The carboxyl stretching frequencies move toward low frequency in comparison with the uncoordinated carboxylate (1700–1740 $cm^{-1}$) in consequence of the carboxylate interaction with metal ion.[6i] In addition, the stretching vibrations $\nu(CH_2)$ in **6** appear at 1437 $cm^{-1}$, and the existence of C–O bonds in **6** gives rise to the peaks at 1110 and 1000, which indicates the grafting of organic groups onto the surface of POM. The bands at 3547–3033 $cm^{-1}$ with strong strength are probably the result of the stretching vibrations ν(H–O) and ν(N–H).

## $^{31}P$ NMR spectroscopic characterization

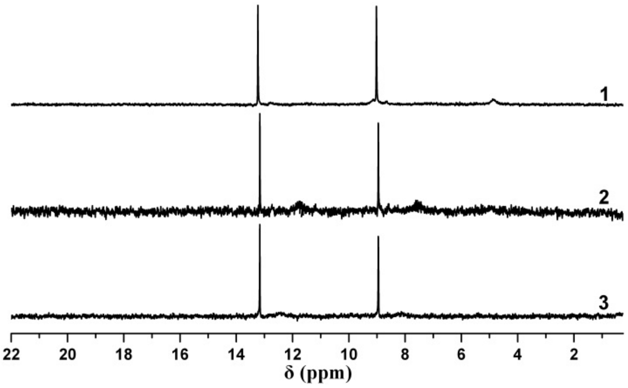

**Fig. 4** $^{31}P$ NMR spectra of **1–3** dissolved in $D_2O$.

$^{31}$P NMR spectroscopy is a powerful tool to investigate the stability of the phosphomolybdates in solution. Thus, we characterized these species in solution by $^{31}$P NMR spectroscopy for determining whether the structures in the solid state being maintained in solution. The $^{31}$P NMR spectra in $D_2O$ of **1**–**3** (Fig. 4) all present a pair of singlet due to $^1$H coupling located at 9.02 and 13.23 ppm ($^1J_{PH}$ = 681.6 Hz), 8.95 and 13.16 ppm ($^1J_{PH}$ = 681.6 Hz), 8.95 and 13.16 ppm ($^1J_{PH}$ = 681.6 Hz), respectively. In addition, the $^{31}$P NMR spectrum of freshly prepared solution of $H_3PO_3$ with $(NH_4)_6Mo_7O_{24}\cdot4H_2O$ (Fig. S4, ESI) is similar to those of crystals of **1**–**3** in $D_2O$, indicating the coordinated carboxylates have no effect on the chemical shifts. In contrast, the $^{31}$P NMR spectra of **4** and **5** in $D_2O$ both present two pairs of singlet (Fig. 5). The decoupled $^{31}$P NMR spectra of **4** and **5** (Fig. S5, ESI) both show the expected two singlets located at 8.54 and 10.94 ppm, 8.86 and 11.04 ppm, respectively, in which the two singlets observed in the NMR spectra are consistent with the presence of two species in solution. Furthermore, the chemical shift located at 8.54 or 8.86 ppm is close to the previously reported phosphomolybdates,[4b,7a] thus showing that the $\{Mo_6\}$ ring is partially stable in **4** and **5**. However, the $^{31}$P NMR spectrum of **6** in $D_2O$ changes rapidly with time (Fig. 6). The solution of **6** indicates degradation form two species to one species within 1 h. The decoupled $^{31}$P NMR spectra of **6** after degradation show the expected one singlet located at 5.82 ppm (Fig. S6, ESI). As described above, **1–6** are not stable in solution and no resonance can be attributed to free phosphite (Fig. S7, ESI).

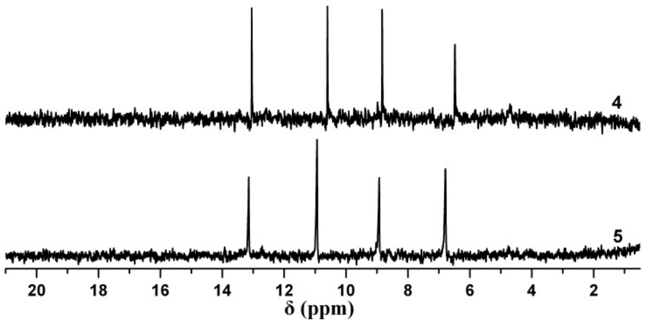

**Fig. 5** $^{31}$P NMR spectra of **4** and **5** dissolved in $D_2O$.

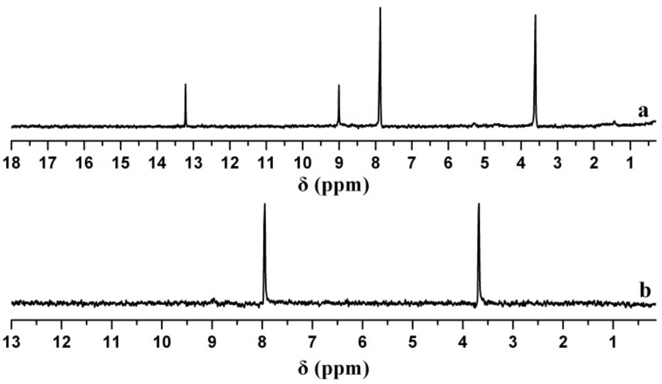

**Fig. 6** $^{31}$P NMR spectra of **6** dissolved in $D_2O$. a) Freshly prepared solution of **6**; b) The solution was placed in the air for less than 1 h.

## XPS and EPR Spectra

The XPS spectra of compounds **1**–**6** (Fig. S8, ESI) in the energy regions of $P_{2p}$ show peaks at 133.1, 133.2, 133.4, 133.0, 133.4 and 132.7 eV respectively, which are not much different from sodium phosphite (133.8 eV) (Fig. S9, ESI), attributed to $P^{3+}$. The XPS spectra of **1**–**6** for Mo atoms exhibit two peaks with binding energies of 232.4 and 235.5 eV for **1**, 232.6 and 235.8 eV for **2**, 232.7 and 235.8 eV for **3**, 232.7 and 235.8 eV for **4**, 232.7 and 235.8 eV for **5**, 232.0 and 235.1 eV for **6** (Fig. S10, ESI), attributing to $Mo^{6+}(3d_{5/2})$ and $Mo^{6+}(3d_{3/2})$ respectively.[11] Compounds **4** and **5** show the thermochromism after heating in the air. With increasing temperature, both compounds could change color form white to dark blue. Taking **5** as an example, notice that, for the heating durations of more than 7 h at 453K, **5** completely changed from white to dark blue (almost black) coloration under atmosphere. The color change was suggested the reduction of metal centers. The following EPR and XPS experiments performed for the heating powder **5** gave us some evidence of the reduced species. EPR spectrum of **5** recorded after heating 7 h at 453K is characteristic of the signatures incorporating $Mo^V$ ion with g-values of g1 = 2.007 and g2 = 1.923 (Fig. S11, ESI).[12] In addition, the major fraction of molybdenum species had binding energies of 235.0 eV ($3d_{3/2}$) and 231.9 eV ($3d_{5/2}$), attributable to $Mo^V$ (Fig. 7).[11]

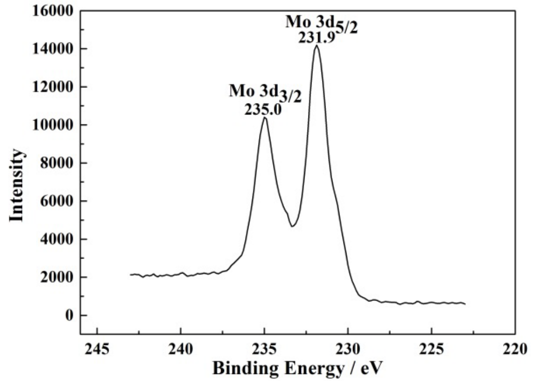

**Fig. 7** XPS spectrum of reduced sample **5** for Mo 3d.

## Conclusions

In summary, we report a strategy providing ligand-accessible coordination sites to direct relevant modular assemblies, in constructing a new family of POM architectures which consist of the common $[HPMo_6O_{21}]^{2-}$ cluster. The coordinated organic ligands play an important templated role in the formation of polyanions and participate directly to their stabilization. These architectures have also displayed that the structural types of the above polyanions can accommodate various carboxylate/alcoholate ligands. The ease of substitution of oxygen-containing organic ligand and heteroatom suggests that other type of polyanions can be similarly synthesized, promising a richer set of architectures in this class. Moreover, the compounds show the interesting thermochromism after heating in the air. Therefore, we present a simple, cheap, and efficient approach, which can easily and systematically synthetize hybrids at different sites.

## Acknowledgements

We gratefully acknowledge financial support from the National Natural Science Foundation of China, the Foundation of Education Department of Henan Province and Natural Science Foundation of Henan Province for financial support.

## Notes and references

[a] Henan Key Laboratory of Polyoxometalate, Institute of Molecular and Crystal Engineering, College of Chemistry and Chemical Engineering, Henan University, Kaifeng 475004, Henan, China.
[b] College of Chemistry and Chemical Engineering, Engineering Research Center of Functional Material Preparation, Shangqiu Normal University, Shangqiu, 476000, Henan, China.

Electronic Supplementary Information (ESI) available: Additional structural figures; the figures of XPS spectra, UV spectra, $^{31}$P NMR spectra and IR spectra. See DOI: 10.1039/b000000x/

1 (a) P. Gouzerh, A. Proust, *Chem. Rev.*, 1998, **98**, 77; (b) A. Dolbecq, E. Dumas, C. R. Mayer, P. Mialane, *Chem. Rev.*, 2010, **110**, 6009; (c) H. N. Miras, J. Yan, D.-L. Long, L. Cronin, *Chem. Soc. Rev.*, 2012, **41**, 7403; (d) A. Müller, P. Gouzerh, *Chem. Soc. Rev.*, 2012, **41**, 7431; (e) A. Banerjee, B. S. Bassil, G.-V. Röschenthaler, U. Kortz, *Chem. Soc.Rev.* 2012, **41**, 7590; (f) A. Proust, B. Matt, R. Villanneau, G. Guillemot, P. Gouzerha, G. Izzet, *Chem. Soc. Rev.*, 2012, **41**, 7605.

2 C. Sanchez, F. Ribot, *New. J. Chem.*, 1994, **18**, 1007.

3 (a) Y.-F. Song, R. Tsunashima, *Chem. Soc. Rev.*, 2012, **41**, 7384; (b) A. Proust, R. Thouvenot, P. Gouzerh, *Chem. Commun.*, 2008, 1837; (c) D.-L. Long, R. Tsunashima, L. Cronin, *Angew. Chem. Int. Ed.*, 2010, **49**, 1736; (d) S. Gatard, S. Blanchard, B. Schollhorn, P. Gouzerh, A. Proust, K. Boubekeur, *Chem. Eur. J.*, 2010, **16**, 8390; (e) K. Hakouk, O. Oms, A. Dolbecq, H. E. Moll, J. Marrot, M. Evain, F. Molton, C. Duboc, P. Deniard, S. Jobic, P. Mialane, R. Dessapt, *Inorg. Chem.*, 2013, **52**, 555.

4 (a) U. Kortz, M. G. Savelieff, F. Y. Abou Ghali, L. M. Khalil, S. A. Maalouf, D. I. Sinno, *Angew. Chem. Int. Ed.*, 2002, **41**, 4070; (b) U. Kortz, J. Vaissermann, R. Thouvenot, P. Gouzerh, *Inorg. Chem.*, 2003, **42**, 1135.

5 (a) U. Kortz, M. T. Pope, *Inorg. Chem.*, 1995, **34**, 2160; (b) U. Kortz, *Inorg. Chem.*, 2000, **39**, 625; (C) L. Yang, Z. Zhou, P. T. Ma, J. P. Wang, J. Y. Niu, *CrystEngComm*, 2013, **15**, 5452.

6 (a) M. Inoue, T. Yamase, *Bull. Chem. Soc. Jpn.*, 1995, **68**, 3055; (b) G. Liu,; S. W. Zhang, Y. Q. Tang, *Z. Anorg. Allg. Chem.*, 2001, **627**, 1077; (c) X. He, J. W. Ye, J. N. Xu, Y. Fan, L. Wang, P. Zhang, Y. Wang, *J. Mol. Struct.*, 2005, **749**, 9; (d) M. Cindrić, T. K. Novak, S. Kraljević, M. Kralj, B. Kamenar, *Inorg. Chim. Acta.*, 2006, **359**, 1673; (e) E. Cartuyvels, K. Van Hecke, L. Van Meervelt, C. Görller-Walrand, T. N. Parac-Vogt, *J. Inorg. Biochem.*, 2008, **102**, 1589; (f) B. Modec, J. V. Brenčič, D. Dolenc, J. Zubieta, *Dalton Trans.*, 2002, 4582; (g) B. Modec, J. V. Brenčič, E. M. Burkholder, J. Zubieta, *Dalton Trans.*, 2003, 4618; (h) B. Modec, D. Dolenc, J. V. Brenčič, J. Koller, J. Zubieta, *Eur. J. Inorg. Chem.*, 2005, 3224; (i) B. Modec, D. Dolenc, M. Kasunič, *Inorg. Chem.*, 2008, **47**, 3625; (j) B. Salignac, S. Riedel, A. Dolbecq, F. Sécheresse, E. Cadot, *J. Am. Chem. Soc.*, 2000, **122**, 10381; (k) J.-F. Lemonnier, S. Floquet, J. Marrot, E. Terazzi, C. Piguet, P. Lesot, A. Pinto, E. Cadot, *Chem. Eur. J.*, 2007, **13**, 3548; (l) J.-F. Lemonnier, S. Floquet, A. Kachmar, M.-M. Rohmer, M. Bénard, J. Marrot, E. Terazzi, C. Piguet, E. Cadot, *Dalton Trans.*, 2007, 3043; (m) J.-F. Lemonnier, A. Kachmar, S. Floquet, J. Marrot, M.-M. Rohmer, M. Bénard, E. Cadot, *Dalton Trans.*, 2008, 4565; (n) E. Cadot, F. Sécheresse, *Chem. Commun.*, 2002, 2189; (o) C. du Peloux, P. Mialane, A. Dolbecq, J. Marrot, F. Sécheresse, *Angew. Chem. Int. Ed.*, 2002, **41**, 2808; (p) W. B. Yang, C. Z. Lu, X. Lin, H. H. Zhuang, *Inorg. Chem.*, 2002, **41**, 452; (q) G. Liu, S. W. Zhang, Y. Q. Tang, *J. Chem. Soc. Dalton Trans.*, **2002**, 2036; (r) Z. H. Zhou, S. Y. Hou, Z. X. Cao, K. R. Tsai, Y. L. Chow, *Inorg. Chem.*, 2006, **45**, 8447; (s) G. G. Gao, L. Xu, X. S. Qu, H. Liu, Y. Y. Yang, *Inorg. Chem.* 2008, **47**, 3402.

7 (a) D. H. Yang, S. Z. Li; P. T. Ma, J. P. Wang, J. Y. Niu, *Inorg. Chem.*, 2013, **52**, 8987; (b) D. H. Yang, S. Z. Li; P. T. Ma, J. P. Wang, J. Y. Niu, *Inorg. Chem.*, 2013, **52**, 14034; (c) D. H. Yang, Y. F. Liang, P. T. Ma, S. Z. Li; J. P. Wang, J. Y. Niu, *Inorg. Chem.*, 2014, **53**, 3048.

8 (a) M. Cindrić, N. Strukan, M. Devčić, B. Kamenar, *Inorg. Chem. Commun.*, 1999, 2, 558; (b) L. L. Li, B. Liu, G. L. Xue, H. M. Hu, F. Fu, J. W. Wang, *Cryst. Growth Des.***,** 2009, **9**, 5206.

9 S. T. Zheng, J. Zhang, X. X. Li, W. H. Fang, G. Y. Yang, *J. Am. Chem. Soc.*, 2010, **132**, 15102.

10 P. F. Wu, P. C. Yin, J. Zhang, J. Hao, Z. C. Xiao, Y. G. Wei, *Chem. Eur. J.*, 2011, **17**, 12002.

11 (a) G. Ilangovan, K. C. Pillai, *Langmuir.*, 1997, **13**, 566; (b) Y. F. Chen, G. S. Yu, F. Li, *Inorg. Chem.*, 2013, **52**, 7431.

12 (a) M. Koziezł, R. Podgajny, R. Kania, R. Lebris, C. Mathonière, K. Lewiński, K. Kruczała, M. Rams, C. Labrugère, A. Bousseksou, B. Sieklucka, *Inorg. Chem.*, 2010, **49**, 2765; (b) C. Baffert, J. F. Boas, A. M. Bond, P. Kçgerler, D.-L. Long, J. R. Pilbrow, L. Cronin, *Chem. Eur. J.*, 2006, **12**, 8472.